Optical and Extreme UV Studies of Spin Dynamics in Metallic and Insulating Ferrimagnets

H. Liu,[1] R. Knut,[2] S. Saha,[2] R. S. Malik,[2] K. Jatkar,[2] R. Stefanuik,[2] J. Söderström,[2] J.E. Shoup,[1] Durga Khadka,[3] T.R. Thapaliya,[3] S.X. Huang,[3] A. Gupta,[4] O. Karis,[2] D. Karaiskaj,[1,*] and D.A. Arena[1,†]

[1]*Department of Physics, University of South Florida, Tampa, Florida 33620, USA*

[2]*Department of Physics and Astronomy, Uppsala University, Box 516, SE-751 20, Uppsala, Sweden*

[3]*Department of Physics, University of Miami, Coral Gables, Florida 33124, USA*

[4]*Center for Materials for Information Technology, The University of Alabama, Tuscaloosa, AL 35487, USA*

(Dated: 01 October 2021)

ABSTRACT

We present all-optical studies of spin dynamics in two classes of ferrimagnets. Both sets of experiments use table-top laser based pump-probe techniques to examine the ultrafast and longer timescale spin excitations. We use visible / near infra-red time-resolved magneto-optical Kerr effect (tr-MOKE) to follow the spin dynamics of a series of metallic $(FeCo)_{1-x}Gd_x$ thin films with varying Gd content. Magnetic compensation in the films occurs at a Gd concentration of ≈26% and the spin dynamics of the films exhibit a non-monotonic variation in effective magnetization. We also examine spin dynamics in an insulating $NiFe_2O_4$ spinel using ultrafast techniques up at extreme ultraviolet energies, which permit element-specific investigations. The element and time-resolved delay scans reveal a non-trivial interaction between spin excitations on the different magnetic sub-lattices of the magnetic insulator.

Introduction

Interest in ferrimagnetic materials has recently grown considerably as ferrimagnets have unique properties with important spintronic applications [1]. The properties of ferrimagnets relevant to spintronics, including the saturation magnetization, spin polarization, and anisotropy, can be tuned across a wide range. The high-frequency properties of ferrimagnets are widely studied, as ferrimagnets combine some of the attractive aspects of high-frequency applications of anti-ferromagnets with the convenience of a net magnetic moment for alignment. In addition, insulating

ferrimagnets are versatile platforms for exploring the physics and applications of pure spin currents in the absence of charge transport [2–5]. Of particular interest of all ferrimagnetic systems are the spin dynamics at ultrafast timescales, which are conveniently probed with laser-based optical techniques. A noteworthy and closely related phenomenon in RE / TM alloys is the non-thermal reversal of magnetization following an ultrafast optical excitation, also referred to as all optical magnetization switching [6, 7].

In this report, we examine two classes of thin film ferrimagnets: $(FeCo)_{1-x}Gd_x$ amorphous metallic alloys and insulating $NiFe_2O_4$ oxides. Both are characterized by competing ferromagnetic and anti-ferromagnetic interactions among different sub-lattices that give rise to a net ferrimagnetic moment but the origins of the interactions are quite distinct. In rare-earth / transition metal alloys such as $(FeCo)_{1-x}Gd_x$, on the rare-earth atoms the intra-atomic exchange integrals favor ferromagnetic alignment between the spin moments on the $4f$ orbitals, positioned several eV away from the Fermi level, and the less than half filled $5d$ electrons that comprise the conduction band. Hybridization between the rare-earth $5d$ states and the Fe, Co $3d$ electrons promotes anti-parallel alignment of the transition metal and Gd moments [2]. The net macroscopic moment can point either in the direction of the Gd or the Fe,Co moments, depending on which sublattice has the larger total moment. The ratio of Gd total moment to the Fe, Co total moment can be adjusted either by changing the Gd content x or by varying the temperature. In the discussion below, FeCo rich (Gd rich) refers to samples where the total moment from the Fe,Co is larger than the corresponding moment from the Gd (Fe,Co) atoms.

In spinel oxides such as $NiFe_2O_4$, the competing spin interactions occur instead between lattice sites with dissimilar point group symmetry, specifically octahedral (O_h) and tetrahedral (T_d) arrangements of oxygen ions surrounding a central transition metal cation [8–11]. Superexchange interactions between the cations, mediated by the intervening oxygen ions, favor anti-parallel spin alignment between the O_h and T_d sites and parallel spin configurations within the O_h and T_d sublattices [12]. The spinel film studied in this work is $NiFe_2O_4$, an inverse spinel containing Ni^{2+} and Fe^{3+} cations. The Fe^{3+} population is evenly split between anti-ferromagnetically aligned O_h and T_d sublattices and hence the net macroscopic moment arises from only the Ni^{2+} spins on the O_h sites.

We present below all-optical studies of spin dynamics in $(FeCo)_{1-x}Gd_x$ and $NiFe_2O_4$ films probed with complementary pump-probe techniques. When an ultrashort laser pulse interacts with an ordered ferromagnetic material, the angular momentum of the system is redistributed between the electron, lattice and spin systems [13]. As a result, the magnetic moment of the

system quenched rapidly and ultrafast demagnetizaton is occurred within ≈ 200 fs. Following the demagnetization, the electronic charges and spins start to relax. This relaxation occurs in two different time scales (≈few ps to ns). The fast relaxation occurs within a few ps time scale due to the exchange of heat between electron, spin and lattice system. The slow relaxation occurs in hundreds to ns time scale due to the diffusion of heat from the electron and lattice system to the surroundings (including the substrate). In addition, at timescales much longer than the initial demagnetization, oscillations in the magneto-optical signal can develop as the rapid heating of the spin system and changes to the sample anisotropy can lead to precessional oscillations of the magnetization [14]. Spin dynamics in the $(FeCo)_{1-x}Gd_x$ system are investigated with time-resolved magneto-optical Kerr effect (tr-MOKE) measurements using ultrafast (*ca.* 50 fs) laser pulses in the visible / near IR spectrum while for the $NiFe_2O_4$studies we use a vis/NIR pump and extreme UV probe. As the low energy magneto-optical response of the $(FeCo)_{1-x}Gd_x$ films is determined by the spin polarization near the Fermi level, the dominant magnetic sublattice is probed with the magneto-optical Kerr effect (MOKE) and the net spin dynamics can be tracked with time-resolved MOKE (tr-MOKE) using visible / near IR light. Conversely, the $NiFe_2O_4$ films are insulating and use of an ultrafast extreme ultraviolet (EUV) probe with sufficient energies to excite the Fe, Ni $M_{2,3}$ core levels permits discrimination between the response of the Ni and Fe spins.

Visible / Near-IR tr-MOKE studies of $(FeCo)_{1-x}Gd_x$ Films

The $(FeCo)_{1-x}Gd_x$ films with a nominal sample structure of Si (substrate) / native SiO_2 layer / $(FeCo)_{1-x}Gd_x$ [100]/ SiO_2 [5] / Pt [1] (numbers in brackets denote thickness in nm) were grown via off-axis DC magnetron sputtering with a stationary substrate. The growth method permitted the development of a film with a near-uniform thickness and with a gradient of the Gd concentration (x) of ≈0.5% per mm along the film. We selected an Fe/Co ratio of ∼8:1 and and the film was diced into sections with differing average Gd concentration (see Fig. 1-a). The Gd concentration at the center of each section was determined with energy dispersive spectroscopy (EDS) excited by a tightly focused scanning electron microscope beam. Repeated EDS measurements were made at or near the center of each section and the atomic Gd concentration at the center of the sections varied from 14 % to 38% with an error estimated to be within 0.5% - 1%. We note that while our (FeCo)Gd films are relatively thick, a small amount of Gd oxidation at the interfaces with the SiO_2 layers may occur [15]; this is not expected to significantly affect the magnetization dynamics presented below.

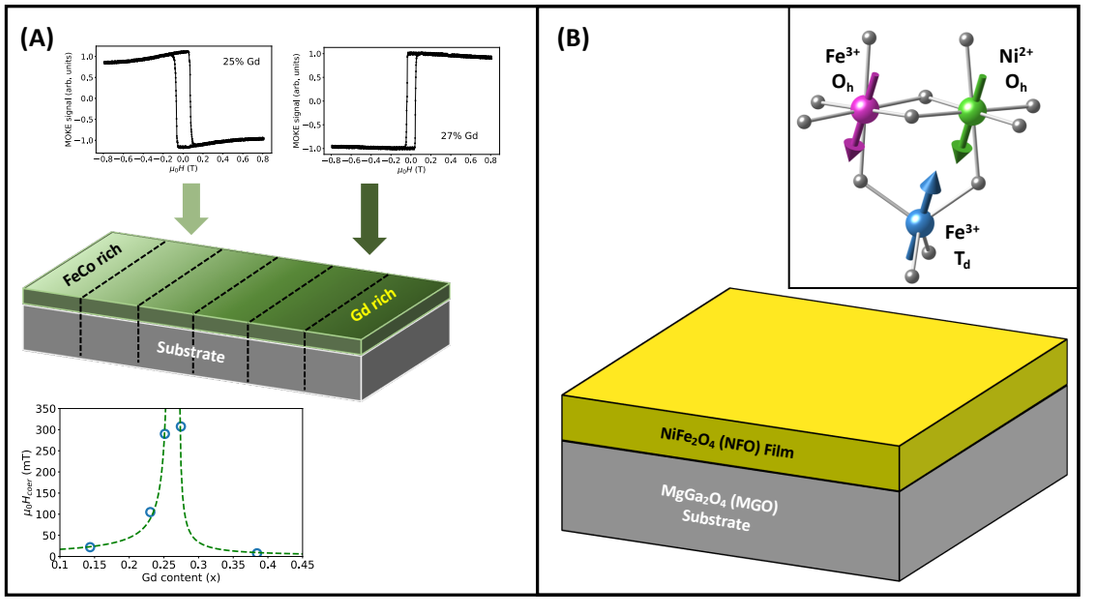

FIG. 1. (a) Combinatorial $(FeCo)_{1-x}Gd_x$ sample grown via off-axis magnetron sputtering. The $(FeCo)_{1-x}Gd_x$ thin film (∼100 nm) is grown on a Si substrate with a gradient of the Gd concentration and then diced into sections with differing average Gd content (dashed lines). Top row: In static MOKE measurements, a reversal of the magneto-optic signal from the FeCo-rich side to the Gd rich side indicates the rare earth - transition metal film progresses through magnetic compensation at room temperature as the Gd concentration increases. Bottom graph: Coercive field ($\mu_0 H_c$) of the samples in mT (blue circles) measured for the in-plane configuration. A divergence of $\mu_0 H_c$ is apparent at the room-temperature compensation point of ∼26% Gd fraction. The green dashed lines are a guide to the eye. (b) The $NiFe_2O_4$ (NFO) film on the isostructural $MgGa_2O_4$ (MGO) substrate, grown via pulsed laser deposition, is an ideal ferrimagnet to investigate dynamical spin interactions between local moments on O_h and T_d sites (inset).

The insets at the top of Fig. 1-a show room-temperature conventional (static) MOKE hysteresis loops recorded in a longitudinal configuration with 632 nm light at the center of the different sections of the gradient sample. The square loops are consistent with an in-plane remanent magnetization; also, x-ray diffraction (not shown) of similarly prepared samples indicates an amorphous crystal structure that results in a negligible in-plane anisotropy. A reversal of the loops (reflection about the $\mu_0 H = 0$ axis) occurs between the 25% Gd and 27% Gd samples. In these metallic samples, the density of states at the Fermi level is dominated by the FeCo $3d$ states and the reversal of the MOKE signal indicates that for the FeCo rich samples the spin polarization of the $3d$ states is aligned with the external field but as more Gd is incorporated into the alloy film the spin polarization of the $3d$ states becomes anti-aligned with the field. That is, below 25% Gd content the total FeCo moment dominates over the total Gd moment and by increasing the Gd content to 27%

the system transitions to one where the total moment from the Gd surpasses the transition metal moments. The Gd spins align with the field and the FeCo moments are anti-aligned, leading to the reversed curve. The static MOKE loops suggest that the system undergoes room temperature magnetic compensation between a Gd content of 25% to 27%. To confirm this effect, we plot in the lower inset to Fig. 1-a the coercive field $\mu_0 H$ in mT for different Gd concentrations. A divergence of $\mu_0 H$ is apparent for a Gd content of about 26%, consistent with the reversal of the hysteresis loops in a similar range of Gd concentration.

We utilize tr-MOKE in a longitudinal configuration to examine the average spin dynamics of the $(FeCo)_{1-x}Gd_x$ samples as a function of Gd content and applied field. Our tr-MOKE apparatus consists of a a pulsed Ti-sapphire regenerative amplifier operating at a repetition rate of 1 kHz and producing ∼100 fs pulses with a central wavelength of 800 nm. This beam was split into the pump and probe beams with the pump beam frequency doubled up to 400 nm to facilitate discrimination of the pump and probe. The linearly polarized beams had fluences of $\sim 0.4\ ^{mJ}/_{cm^2}$ and $\sim 0.075\ ^{mJ}/_{cm^2}$, respectively, for the pump and probe beams. After reflection off the sample, the Kerr rotation was monitored by passing the beam through a $\lambda/2$ plate. A Wollaston prism was used to split the reflected beam into the s and p components, which were subsequently detected with a balanced Si photodetector. Care was taken to ensure spatial overlap of the pump and probe beams, with the area of the probe reduced by 3× relative to the pump. A mechanical stage was used to vary the time delay between the pump and probe beams. The variable magnetic field was produced by an external electromagnet with the field axis rotated 20° away from the in-plane direction. The out-of-plane tilt angle is necessary to efficiently observe coherent spin precession as the field component normal to the sample surface pulls the magnetization away from the film plane, resulting in a magnetization vector that is slightly canted out of plane. Upon heating by the ultrafast pump pulse, both the magnitude of the magnetization and the anisotropy, including the shape anisotropy, are rapidly modified, resulting in a new equilibrium canting angle. As the magnetization vector initially remains pointing along the original canting angle, the system begins to precess coherently around the new canting angle, resulting in an oscillatory tr-MOKE signal as a function of delay time [14]. However, we note that the initial 20° applied field direction away from the film plane is sufficiently small that the net magnetization retains a dominant in-plane character.

Representative tr-MOKE scans of the 23% Gd and 27% Gd samples as a function of applied field are presented in Fig. 2-a. Delay times $t < 0$ represent the equilibrium state of the system with the magnetization oriented slightly out-of-plane. At $t = 0$, that is, the temporal overlap of

pump and probe beams, there is a discontinuity of the tr-MOKE signal indicative of an ultrafast demagnetization of the $(FeCo)_{1-x}Gd_x$ film. After the initial demagnetization the tr-MOKE signal decreases in amplitude and begins a return to its equilibrium value, however for $t \gtrsim 20$ ps an oscillatory signal develops, superposed on the decay back towards equilibrium. The discontinuity at $t = 0$ clearly reverses sign as the Gd content increases from 23% to 27%, consistent with the static MOKE loops shown in Fig. 1-a and again indicating that the magnetization of the system transitions from FeCo to Gd dominant as the Gd content increases. The field dependent traces also exhibit an increase in the oscillation frequency with increasing field.

The oscillations for $t \gtrsim 20$ ps arise from the significant perturbation in the magnetization initiated by the strong pump pulse. The pump pulse quickly heats up the sample which in turn reduces the magnetization M. In addition, the anisotropy of the film can change with temperature and this effect has been observed in rare-earth / transition metal films [16–21]. Both effects (magnetization and anisotropy variations following the pump pulse) result in a modified equilibrium orientation of the magnetization, and the net magnetization begins to precess around the new equilibrium axis. Even after the heat dissipates away from the excitation area, the magnetization continues to precess until eventually damping processes cause the magnetization to relax back towards the original equilibrium direction. We note that by the time the precessional oscillations develop an appreciable amplitude, any transient rise in the electronic or lattice temperature has dropped to well below the Curie temperature [7].

We extract the frequency of the oscillations for the samples at different applied fields with a damped sinusoidal oscillation model superposed on a decaying exponential (black solid or dashed lines in Fig. 2-a):

$$I(t) = A_b\, e^{-t/\tau_b} + A_s\, \sin(\omega t + \phi)\, e^{-t/\tau_s} \tag{1}$$

Here, $I(t)$ is the tr-MOKE signal, A_b is the amplitude of the background with time constant τ_b, A_s is the amplitude of the damped precessional oscillations with frequency ω and damping time τ_s; ϕ is an arbitrary phase determined from the start of the time window for the fit. The resulting freq. vs. field data sets for samples with different Gd content are presented in Fig. 2-b. At a given field, the precession frequency tends to decrease with increasing Gd content, but the trend is not monotonic. The ordering of the different films from highest frequency to lowest jumps around a bit as a function of field, but can be characterised as (14%, 25%, 27%, 23%, 38%) for the lower range of applied fields ($\mu_0 H < 0.45$ T) while at higher fields the ordering is closer to (14%, 25%,

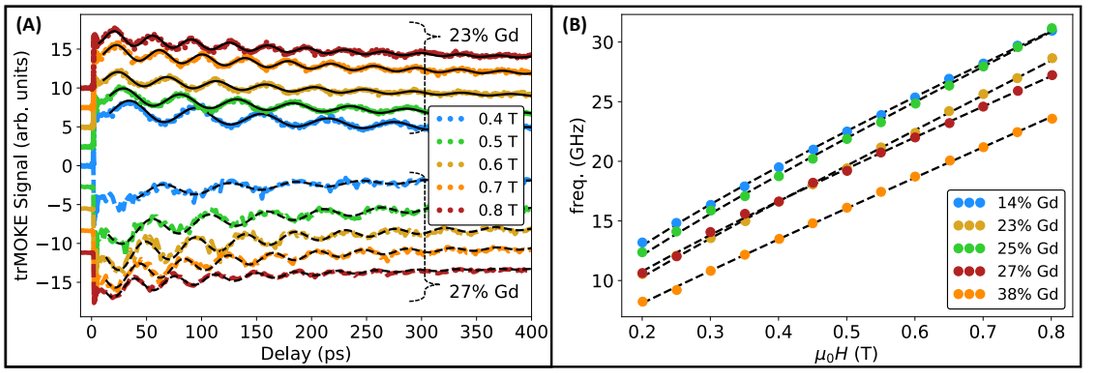

FIG. 2. (a) tr-MOKE traces of demagnetization, recovery and ferromagnetic resonance (FMR) behavior for two Gd concentrations. Pump and probe pulses overlap at $t = 0$ and the reversal in the sign of the tr-MOKE trace for $t > 0$ indicates a transition from (FeCo) dominant spins (23% Gd) to Gd dominant spins (27% Gd). The FMR oscillations are evident for $t > 20$ ps and the black solid or dashed lines are fits to Eq. 1. tr-MOKE traces for $\mu_0 H > 0.4$ T are offset vertically for clarity. (b) Frequency (GHz) vs. applied field ($\mu_0 H$) for the different $(FeCo)_{1-x}Gd_x$ films. The dashed lines are fits to the Kittel equation (Eq. 2). The non-monotonic behavior of the films for Gd concentration x between 23% and 27% is evident.

23%, 27%, 38%).

As mentioned above, the precessional motion of the magnetization is equivalent to ferromagnetic resonance (FMR) and we analyze the frequency vs. field behavior with the well-known Kittel relationship for in-plane resonance [22]:

$$f = \frac{\gamma}{2\pi}\mu_0\sqrt{(H_{app}) \times (H_{app} + M_{eff})} \tag{2}$$

Here, f is the resonance frequency extracted from the tr-MOKE data, γ is the gyromagnetic ratio, H_{app} is the applied field, and M_{eff} is the effective magnetization which includes contributions from the sample anisotropy and demagnetization fields. The dashed lines in Fig. 2-b are fits to Eq. 2.

The extracted values for $\mu_0 M_{eff}$ are [1.19, 0.46, 0.77, 0.82, 0.32] (values in Tesla) for the (14%, 23%, 25%, 27%, 38%) samples, respectively. Clearly, $\mu_0 M_{eff}$ does not vary monotonically with increasing Gd content. Several factors account for this non-trivial variation in effective magnetization. First, as revealed by the direction of the static hysteresis loops, the as the Gd content increases, room-temperature magnetization compensation occurs for a Gd concentration near 25% - 26%. The effective magnetization at room temperature is expected to dip and then increase as more Gd is incorporated into the film. Second, the effective magnetization contains contributions from

the saturation magnetization and also anisotropy fields in the sample. In the concentration range studied, $(FeCo)_{1-x}Gd_x$ films are amorphous with little in-plane anisotropy and hence to first order, the anisotropy contribution to effective magnetization can be expressed as $M_{eff} = M_s - 2K_U^{\perp}/\mu_0 M_s$, where M_S is the volume magnetization and $K_U^{\perp}$ is the out-of-plane uniaxial anisotropy constant. High-sensitivity transverse AC magnetic susceptibility measurements reveal that RE / TM alloys can exhibit one or more spin reorientation transitions [16]. In Fe-Gd samples with a fixed composition and a similar thickness to the films studied here, the effective anisotropy can switch between in-plane to out-of-plane as a function of temperature, and the crossover between in-plane to out-of-plane easy axis does not always coincide with the magnetization compensation temperature [16].

Our $(FeCo)_{1-x}Gd_x$ samples with a spatial gradient in the Gd content may thus display a complicated variation in not only the magnetization but also the anisotropy. Additional tr-MOKE scans as a function of applied field direction, while maintaining a saturated magnetic state and illuminating the same spot on the sample with the pump and probe, will clarify the interplay between the two parameters. Nonetheless, the results presented again illustrate the utility of tr-MOKE in studying the high-frequency dynamics of ferrimagnetic systems. Of course in ferrimagnets, it would be of great value to examine the dynamics of individual magnetic sub-lattices. For those studies, we must take advantage of higher-energy probes that can access elemental core levels.

EUV Studies of Spin Dynamics in $NiFe_2O_4$

Oxides with the spinel structure can exhibit widely varying properties such as highly insulating phases, semiconductors, metal to insulator transitions, transparent conductors, and even superconductivity. Spinel ferrites have the general formula XFe_2O_4, where X is a divalent or trivalent metal cation such as Ni, Cu or Zn [23]. Spinel ferrites exhibits different magnetic order including paramagnetic, ferromagnetic, antiferromagnetic, and ferrimagnetic, *etc.* The spinel ferrites can also exhibit various emerging phenomena and complex behavior such as half-metallicity, spin frustration, spin glass formation, and the existence of quantum critical points. As a result spinel ferrites have emerged as a potential candidate for novel spintronics devices.

$NiFe_2O_4$ is one of the insulating ferrimagnetic oxides with an inverse spinel structure. Recently $NiFe_2O_4$ has emerged as a potential candidate to use as a magnetic component in artificial multiferroic heterostructures or as spin filtering tunnel barriers for spintronics devices [24–27]. For application purpose, these structures are grown as a thin film on top of different substrates. The

initial lattice mismatch between the film and the substrate can incorporate a significant amount of strain into the system and strain in the spinel films can alter the magnetic ground state. Strain-driven effects include a significant increase of saturation magnetization [28] and enhanced uniaxial magnetic anisotropy [29, 30]. Strain is also an efficient method to alter magneto-elastic coupling [33] and dramatically decrease damping of spin dynamics [31].

Ni-ferrite ($NiFe_2O_4$) has an inverse spinel structure [32], where the octahedral sites (O_h or B-sites) are randomly occupied by equal number of Ni^{2+} and Fe^{3+} cations. The tetrahedral (T_d or A-sites) are occupied by only Fe^{3+}. The AF coupling between the O_h and T_d sites leads to complete cancellation of the spin moment from the the Fe^{3+} cations and hence the net moment in $NiFe_2O_4$ is derived primarily from the Ni^{2+} cations on the O_h sites. $NiFe_2O_4$ can be synthesized in the bulk as a fully inverse spinel with a cubic lattice parameter of a = 0.8345 nm. In this section we will focus on exploring the element-specific spin-dynamics at ultrafast timescale, in the particular example of a strained, insulating ferrimagnetic thin film. For this purpose we will use a state-of-the-art lab-based advanced laser system that is used as high harmonic generator photon source that provides extreme ultraviolet (EUV $\sim$ 20 – 72 eV) photon pulses with very ultrashort pulse lengths (30 fs).

Element specific magnetization dynamics are measured at the HELIOS laboratory in Uppsala University, Sweden. HELIOS uses the non-linear high harmonic generation (HHG) process to generate ultrashort pulses of extreme ultraviolet (EUV) photons in the range between 40-72 eV [33, 34].Recently, HHG has emerged as a powerful tool to probe the M-edge resonances ($3p$ core levels) in $3d$ transition metals compounds. This capability enables investigation of the element specific response in a multi-sublattice systems such as Heusler alloys [35], ferrimagnetic alloys [36], Co-Pt alloys [37], antiferromagnetically coupled trilayer systems [38], and other systems. The HHG technique is also has used to investigate the optically driven spin-selective charge transfer from one magnetic sublattice to another, which is popularly known as optical inter-site spin transfer (OISTR) effect [39, 40].

In our transverse magneto optical Kerr effect (T-MOKE) [41] set up at HELIOS, the EUV photons are reflected by the sample at 45° angle of incidence, and subsequently measured with a spectrometer as shown in Fig. 3-a. The light is polarized in the plane of incidence to provide a magnetic contrast in the T-MOKE geometry. The T-MOKE end station at HELIOS supplied a field of ±80 mT for the HHG time resolved measurements presented. Any magnetization perpendicular to the plane of incidence will affect the reflectivity of the sample. The change in magnetization is quantified by the magnetic asymmetry which is the difference in reflectivity be-

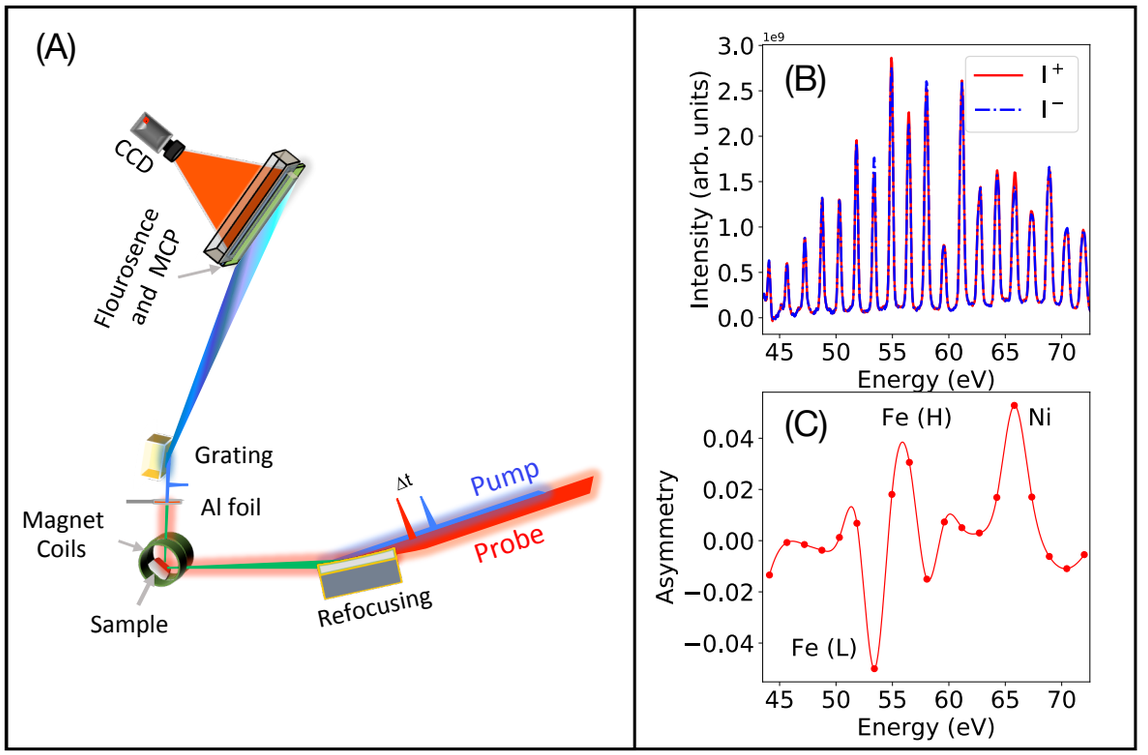

FIG. 3. (a)The schematic of the element specific T-MOKE set up present at Uppsala University (b) High harmonic spectrum of NFO that contains both even and odd harmonics. The red and blue spectra corresponds to positive and negative magnetization direction, respectively. (b) The asymmetry spectrum of NFO, the asymmetry around 66 eV comes from the magnetization of Ni, while the more complex shape between 50-60 eV is due to tetrahedral and octahedral Fe.

tween two opposite magnetization directions (I^+ and I^-), divided by the sum of these reflectivities, $A = {}^{(I^+-I^-)}/_{(I^++I^-)}$. HHG generally provides only the odd harmonics of the fundamental and hence the energy spacing between the odd harmonics is 3.1 eV [42, 43]. By mixing the fundamental with its second harmonic, we also generated even harmonics such that the asymmetry spectrum with twice as many harmonics over the measured energy range could be obtained [44]. This spectrum is shown in Fig. 3-b, where red and blue spectra correspond to I^+ and I^- respectively. The spectrum has a cut-off at 72 eV due to an Al-filter that acts as a band-pass filter which blocks the 1.55 eV fundamental laser light and also photons with energy greater than 72 eV [45].

A 40 nm thin $NiFe_2O_4$ film was grown onto a (100) oriented spinel $MgGa_2O_4$ (MGO) substrate with pulsed laser deposition. The use of an isostructural substrate leads to a $NiFe_2O_4$ film with low anti-phase boundary defects but the lattice mismatch between the substrate and the $NiFe_2O_4$ film leads to a compressive in-plane strain of 0.78 % in the film; our 40 nm film remains coherently

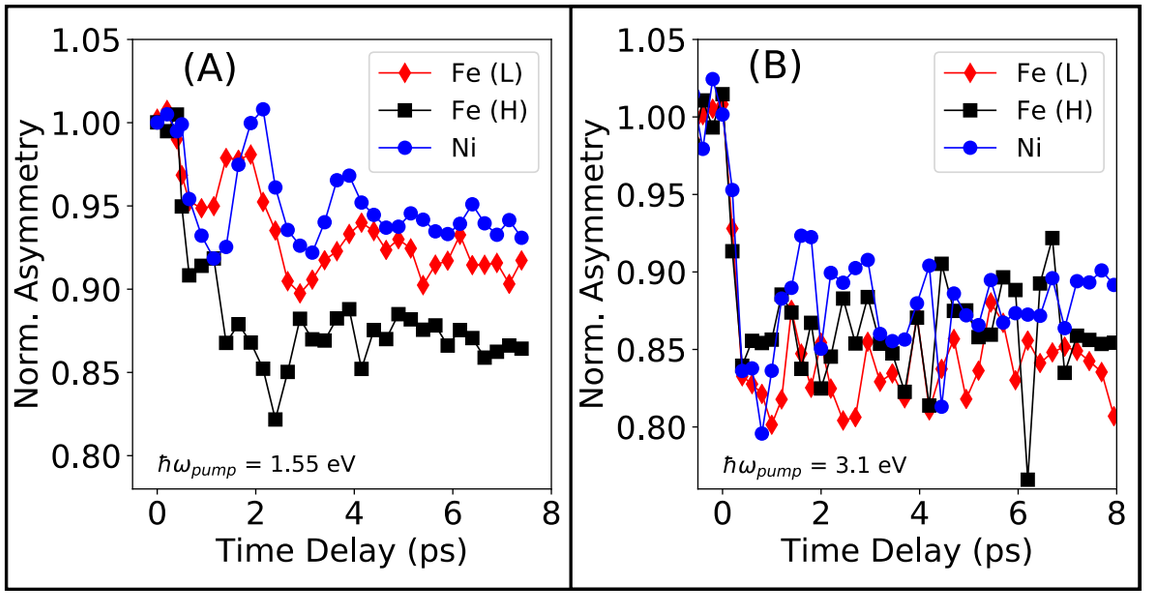

FIG. 4. Time resolved normalized asymmetry at the three different energies indicated in fig.2. (a) Strong oscillations are observed for the Ni and Fe asymmetry, while the the system is pumped with 800 nm laser light (1.55 eV photon energy). (b) No oscillations are observed while the system is pumped with 400 nm laser light (3.1 eV) photon energy. depending on the probing energy.

strained with modified in-plane and out-of-plane lattice parameters. The details film growth process and structural characterization of the film can be found in [46]. The T-MOKE asymmetry spectrum collected at HELIOS is shown in Fig. 3-c. The asymmetry from the Ni cations occupying the O_h sites corresponds to photon energies in the range of 63-72 eV with a maximum value of ≈ 0.05 at 65.8 eV. Contributions from the Fe cations exhibit asymmetry across the 50-60 eV energy range; the Fe spectra contains contributions from both the T_d and O_h sites. The odd harmonics capture the peak asymmetries for both Ni and Fe, where Fe has two strong asymmetries of $\approx$ -0.055 and ≈ 0.031 at 53.4 eV and 56.5 eV respectively. Even though the asymmetry and binding energies between tetrahedral and octahedral sites of Fe should differ, it is not possible to uniquely assign the two Fe asymmetries to the two different Fe sites due to the large spectral overlap between the two Fe species. We will hence refer to the 54 and 57 eV peaks as Fe_L and Fe_H, respectively. However, a reasonable assumption is that the Fe_L asymmetry has a stronger contribution from T_d site of Fe, since its sign is opposite to the Ni asymmetry at 66 eV, corresponding to the antiferromagnetic alignment between tetrahedral Fe and octahedral Ni.

Band structure calculations indicate that $NiFe_2O_4$ is a wide gap insulator with a band gap of 2.4 eV [47]. To distinguish the different contributions to the magnetization dynamics, the sample

is pumped by using two different photon energies, namely 1.55 eV or 3.1 eV, and the spin dynamics are probed using the EUV pulse. For the higher energy 3.1 eV pump, direct excitations across the band gap are possible while the lower energy 1.55 eV pump leads to excitations either from gap states or from the valence band to virtual states in the gap. In addition, the 1.55 eV pump may partially pass through the $NiFe_2O_4$ film and into the substrate. Hence we anticipate distinct spin dynamics when exciting above or below the gap, as can be seen in Fig. 4. For lower energy 1.55 eV, the Ni and the Fe_L and Fe_H spectral features exhibit dissimilar degrees of demagnetization. The demagnetization for Fe_L is much smaller compared to Fe_H while the Ni response is generally the weakest of the three. The demagnetization curve for Fe_H is simpler in comparison to the Fe_L feature. The Fe_L optical response shows a more complex structure where the asymmetry starts to increase after about 0.5 ps and appears to have an oscillatory behavior (red curve). A similar and stronger oscillation is also apparent in the Ni response with a period of $\approx$ 2 ps that is fully damped after 5 ps (blue curve). The asymmetry appears to fully recover at the peak of the first oscillation (A $\approx$ 1) at 1.5 ps. In contrast, when using a higher energy pump of 3.1 eV, as shown in Fig. 4-b, the oscillatory behaviour in the magnetic signal at Ni and Fe_L features is quite difficult to observe. Additionally, the percentage of demagnetization is essentially the same for Ni and the two Fe features and we note that the degree of demagnetization for the Fe_H feature is similar for both the pump pulse energies. The different data sets for 3.1 eV pump are fitted with a three-temperature model and the ultrafast demagnetization time for all the elements are estimated as $\approx$ 130 fs whereas the remagnetization times are much slower.

Metallic systems usually exhibit fast electron scattering and thermalization as there is a large phase space at the Fermi level that can support scattering events. In the case of insulating oxides the electron thermalization can be expected to be significantly slower. The holes created in the valence band after optical excitation can still scatter efficiently, resulting in a fast demagnetization. As mentioned, the $NiFe_2O_4$ band gap is expected to be about 2.4 eV. Hence, the excitations we observe with 1.55 eV may be related to gap states that exist due to defects such as oxygen vacancies. When an oxygen vacancy is created, the excess electrons not transferred to the oxygen anion are redistributed among adjacent cations. For stoichiometric $NiFe_2O_4$, the minority spin t_{2g} orbitals on Ni^{2+} are filled, and therefore any additional electrons must begin to populate the normally empty minority spin e_g level, leading to hybridization of oxygen $2p$ and Ni $3d$ states. This gives rise to an extra state above the valence band [48–50]. This gap state may be excited when we pump with 1.55 eV photons, resulting in the observed ultrafast demagnetization. However, with 3.1 eV pump photons the direct excitation of valence band states into the conduction band becomes

possible. This results not only in a faster demagnetization but as the valence band states are strongly hybridized, one can expect the dynamics to become more similar between the elements, as observed with the 3.1 eV pump.

Summary and Concluding Comments

In summary, we have investigated spin dynamics at room temperature in two different classes of ferrimagnets using ultrafast optical techniques. In the case of the metallic $(FeCo)_{1-x}Gd_x$ thin films, we use tr-MOKE to observe a reversal of the demagnetization signal as the Gd content x is increased, consistent with the transition from a ferrimagnetic state dominated by the (Fe,Co) moments to one where the rare-earth Gd moments align with the external applied field. Analysis of the long time scale ferromagnetic resonance region of the dynamic response reveals a possible complicated interaction between the sample magnetization and the anisotropy of the $(FeCo)_{1-x}Gd_x$ system that evolves in time. For the insulating ferrimagnet $NiFe_2O_4$, we observe a variation of the demagnetization depending on whether the excitation energy is below or above the $NiFe_2O_4$ band gap. Moreover, a high frequency oscillation is apparent in the Ni and Fe_H signal only when the system is pumped below the band gap. While the investigation of these effects is ongoing, the results emphasize the utility of both visible / NIR and element-specific HHG probes of magnetization dynamics in these disparate ferrimagnetic systems.

We conclude with some comments and observations on studies of spin dynamics in ferrimagnets using the tr-MOKE and HHG approaches. Visible / near UV probe pulses in tr-MOKE studies of RE / TM alloy ferrimagnets are useful to directly examine magnetic compensation as the low pump energy does not directly excite the RE $4f$ spins and instead only reveals the spin alignment of the TM $3d$ states. Optical tr-MOKE studies of insulating / semi-conducting oxides and related materials are less common, although there have been reports of tr-MOKE studies of Skyrmion lattice spin dynamics in GaV_4S_8 [51] and related optical techniques such as time resolved Faraday effect employed to examine spin dynamics in Fe_3O_4 / γ-Fe_2O_3 nanoparticles [52].

Experimentally, tr-MOKE offers a number of advantages. The probe pulse can also be tightly focused, which is useful in examining samples with micron-scale inhomogeneities, as occurs in our compositionally graded $(FeCo)_{1-x}Gd_x$ samples. The tight focus can also be combined with prototype magnetic device structures which may enable, for example, studies of spin dynamics of voltage controlled magnetization. The optical set up of tr-MOKE is generally more simple than HHG. Many tr-MOKE table top instruments have an optical path in air, and high repetition rate

Ti:sapphire amplifiers make data collection efficient and relatively fast. The relative simplicity of tr-MOKE more easily permits the incorporation of additional sample environments, such as variable temperature and / or high magnetic fields. Lastly, the exceptional time-resolution of tr-MOKE and related techniques can be used to examine both the ultrafast demagnetization dependence, but also higher-energy spin excitation modes such as THz-scale exchange resonances in anti-ferromagnets and ferrimagnets [53].

Conversely, the high-harmonic generation approach has additional features that are useful for examining multi-component systems such as many ferrimagnets. The ability to directly probe localized, elemental core levels in principle enables a decomposition of spin dynamics by atomic species and hence HHG is a useful complement to more sophisticated approaches such as free electron lasers. HHG studies can examine differential demagnetization and remagnetization times for different elements in a sample [36, 54] and this will be of great use in studying the nature of exchange resonances and other high-frequency modes in ferrimagnets. Combined with a flexible arrangement for the pump pulse energy, the HHG method will provide a unique perspective on the states contributing to ultrafast demagnetization, recovery, and THz-to GHz spin excitations.

The HHG approach, however, is less straightforward to implement than conventional tr-MOKE. Non-linear conversion of the incident laser pulse to the harmonic spectrum is a delicate process, and the low mean free path of extreme UV photons in air imposes the complication of a vacuum path for the EUV harmonics. Moreover, a spectral dispersion of the HHG pulse is necessary to differentiate the harmonics. To date, this has limited HHG studies to more simple sample environments than tr-MOKE, although this is a practical, not fundamental, limitation. A more challenging issue can be the incomplete understanding of elemental resonances in the EUV range and the resulting spectroscopy of lower energy core levels such as the 2^{nd} row transition $M_{2,3}$ edges and the rare earth $O_{2,3}$ and $N_{4,5}$ edges as these low energy core levels are much less studied than their soft x-ray counterparts. Nonetheless, the utility of HHG, and the closely related tr-MOKE approach, ensures that both methods will be indispensable for understanding the spin dynamics of multiple ferrimagnetic systems.

This material is based upon work supported by the National Science Foundation under Grant No. ECCS-1952957. DAA acknowledges the support of the USF Nexus Initiative and the Swedish Fulbright Commission. Work at the University of Alabama is supported by NSF Grant No. ECCS-1509875.

Data availability: The data that support the findings of this study are available from the corresponding author upon reasonable request.

REFERENCES

* e-mail: karaiskaj@usf.edu

† Corresponding author: darena@usf.edu

[1] H. A. Zhou, T. Xu, H. Bai, and W. Jiang, "Efficient spintronics with fully compensated ferrimagnets," *J. Phys. Soc. Japan*, vol. 90, may 2021.

[2] J. Barker and U. Atxitia, "A review of modelling in ferrimagnetic spintronics," *J. Phys. Soc. Japan*, vol. 90, may 2021.

[3] S. Matzen, J.-B. Moussy, P. Wei, C. Gatel, J. C. Cezar, M. A. Arrio, P. Sainctavit, and J. S. Moodera, "Structure, magnetic ordering, and spin filtering efficiency of NiFe 2 O 4 (111) ultrathin films," *Appl. Phys. Lett.*, vol. 104, p. 182404, may 2014.

[4] S. Emori, D. Yi, S. Crossley, J. J. Wisser, P. P. Balakrishnan, B. Khodadadi, P. Shafer, C. Klewe, A. T. N'Diaye, B. T. Urwin, K. Mahalingam, B. M. Howe, H. Y. Hwang, E. Arenholz, and Y. Suzuki, "Ultralow Damping in Nanometer-Thick Epitaxial Spinel Ferrite Thin Films," *Nano Lett.*, vol. 18, pp. 4273–4278, jul 2018.

[5] D. Qu, S. Y. Huang, J. Hu, R. Wu, and C. L. Chien, "Intrinsic Spin Seebeck Effect in Au / YIG," *Phys. Rev. Lett.*, vol. 110, p. 067206, feb 2013.

[6] C. D. Stanciu, F. Hansteen, A. V. Kimel, A. Kirilyuk, A. Tsukamoto, A. Itoh, and T. Rasing, "All-optical magnetic recording with circularly polarized light," *Phys. Rev. Lett.*, vol. 99, jul 2007.

[7] A. Kirilyuk, A. V. Kimel, and T. Rasing, "Laser-induced magnetization dynamics and reversal in ferrimagnetic alloys," *Reports Prog. Phys.*, vol. 76, feb 2013.

[8] E. W. Gorter, "Saturation Magnetization and Crystal Chemistry of Ferrimagnetic Oxides - I," *Philips Res. Reports*, vol. 9, pp. 295–320, 1954.

[9] E. W. Gorter, "Saturation Magnetization and Crystal Chemistry of Ferrimagnetic Oxides - II," *Philips Res. Reports*, vol. 9, pp. 321–365, 1954.

[10] E. W. Gorter, "Saturation Magnetization and Crystal Chemistry of Ferrimagnetic Oxides - III," *Philips Res. Reports1*, vol. 9, pp. 403–443, 1954.

[11] A. Broese van Groenou, P. F. Bongers, A. L. Stuyts, A. van Groenou, P. F. Bongers, and A. L. Stuyts, "Magnetism, microstructure and crystal chemistry of spinel ferrites," *Mater. Sci. Eng.*, vol. 3, pp. 317–392, feb 1969.

[12] Y. Suzuki, "Epitaxial Spinel Ferrite Thin Films," *Annu. Rev. Mater. Res.*, vol. 31, pp. 265–289, 2001.

[13] B. Koopmans, M. Van Kampen, J. T. Kohlhepp, and W. J. De Jonge, "Ultrafast magneto-optics in nickel: magnetism or optics?," *Phys. Rev. Lett.*, vol. 85, pp. 844–847, jul 2000.

[14] M. van Kampen, C. Jozsa, J. T. Kohlhepp, P. LeClair, L. Lagae, W. J. M. de Jonge, and B. Koopmans, "All-Optical Probe of Coherent Spin Waves," *Phys. Rev. Lett.*, vol. 88, pp. 227201/1–227201/4, may

2002.

[15] D. A. Gilbert, J. Olamit, R. K. Dumas, B. J. Kirby, A. J. Grutter, B. B. Maranville, E. Arenholz, J. A. Borchers, and K. Liu, "Controllable positive exchange bias via redox-driven oxygen migration," *Nat. Commun. 2016 71*, vol. 7, pp. 1–8, mar 2016.

[16] A. Chanda, J. E. Shoup, N. Schulz, D. A. Arena, and H. Srikanth, "Tunable competing magnetic anisotropies and spin reconfigurations in ferrimagnetic Fe100-xGdx alloy films," *Phys. Rev. B*, vol. 104, p. 094404, sep 2021.

[17] S. Joo, R. S. Alemayehu, J. G. Choi, B. G. Park, and G. M. Choi, "Magnetic Anisotropy and Damping Constant of Ferrimagnetic GdCo Alloy near Compensation Point," *Materials (Basel).*, vol. 14, p. 2604, may 2021.

[18] E. Kirk, C. Bull, S. Finizio, H. Sepehri-Amin, S. Wintz, A. K. Suszka, N. S. Bingham, P. Warnicke, K. Hono, P. W. Nutter, J. Raabe, G. Hrkac, T. Thomson, and L. J. Heyderman, "Anisotropy-induced spin reorientation in chemically modulated amorphous ferrimagnetic films," *Phys. Rev. Mater.*, vol. 4, p. 074403, jul 2020.

[19] F. Hellman, "Measurement of magnetic anisotropy of ferrimagnets near compensation," *Appl. Phys. Lett.*, vol. 59, p. 2757, jun 1998.

[20] M. Hirscher, T. Egami, and E. E. Marinero, "Atomistic study of magneto-optical amorphous thin films using synchrotron radiation," *J. Appl. Phys.*, vol. 67, no. 9, pp. 4932–4934, 1990.

[21] N. Heiman, A. Onton, D. F. Kyser, K. Lee, and C. R. Guarnieri, "Uniaxial anisotropy in rare earth (Gd, Ho, Tb) -transition metal (Fe, Co) amorphous films," *AIP Conf. Proc.*, vol. 24, pp. 573–574, aug 1975.

[22] S. Azzawi, A. T. Hindmarch, and D. Atkinson, "Magnetic damping phenomena in ferromagnetic thin-films and multilayers," *J. Phys. D. Appl. Phys.*, vol. 50, p. 473001, nov 2017.

[23] J.-B. Moussy, "From epitaxial growth of ferrite thin films to spin-polarized tunnelling," *J. Phys. D. Appl. Phys.*, vol. 46, p. 143001, mar 2013.

[24] N. M. Caffrey, D. Fritsch, T. Archer, S. Sanvito, and C. Ederer, "Spin-filtering efficiency of ferrimagnetic spinels CoFe2O 4 and NiFe2O4," *Phys. Rev. B - Condens. Matter Mater. Phys.*, vol. 87, p. 024419, jan 2013.

[25] U. Lüders, A. Barthélémy, M. Bibes, K. Bouzehouane, S. Fusil, E. Jacquet, J. P. Contour, J. F. Bobo, J. Fontcuberta, and A. Fert, "NiFe2O4: A versatile spinel material brings new opportunities for spintronics," *Adv. Mater.*, vol. 18, pp. 1733–1736, jul 2006.

[26] U. Lüders, M. Bibes, K. Bouzehouane, E. Jacquet, J. P. Contour, S. Fusil, J. F. Bobo, J. Fontcuberta, A. Barthelemy, and A. Fert, "Spin filtering through ferrimagnetic NiFe 2 O 4 tunnel barriers," *Appl. Phys. Lett.*, vol. 88, p. 082505, feb 2006.

[27] C. A. Vaz, J. Hoffman, C. H. Ahn, and R. Ramesh, "Magnetoelectric Coupling Effects in Multiferroic Complex Oxide Composite Structures," *Adv. Mater.*, vol. 22, pp. 2900–2918, jul 2010.

[28] A. B. Schmidt, M. Pickel, M. Donath, P. Buczek, A. Ernst, V. P. Zhukov, P. M. Echenique, L. M.

Sandratskii, E. V. Chulkov, and M. Weinelt, "Ultrafast Magnon Generation in an Fe Film on Cu(100)," *Phys. Rev. Lett.*, vol. 105, p. 197401, nov 2010.

[29] M. Bibes, J. E. Villegas, and A. Barthélémy, "Ultrathin oxide films and interfaces for electronics and spintronics," *Adv. Phys.*, vol. 60, no. 1, pp. 5–84, 2011.

[30] C. La-O-Vorakiat, M. Siemens, M. M. Murnane, H. C. Kapteyn, S. Mathias, M. Aeschlimann, P. Grychtol, R. Adam, C. M. Schneider, J. M. Shaw, H. Nembach, and T. J. Silva, "Ultrafast Demagnetization Dynamics at the M Edges of Magnetic Elements Observed Using a Tabletop High-Harmonic Soft X-Ray Source," *Phys. Rev. Lett.*, vol. 103, p. 257402, dec 2009.

[31] M. I. Katsnelson, V. Y. Irkhin, L. Chioncel, A. I. Lichtenstein, and R. A. de Groot, "Half-metallic ferromagnets: From band structure to many-body effects," *Rev. Mod. Phys.*, vol. 80, pp. 315–378, apr 2008.

[32] R. Knut, R. S. Malik, C. Kons, J. E. Shoup, F. Radu, C. Luo, Y. O. Kvashnin, A. Gupta, O. Karis, and D. A. Arena, "Perpendicular and in-plane hole asymmetry in a strained {NiFe}2O4 film," *J. Phys. Condens. Matter*, vol. 33, p. 225801, may 2021.

[33] S. Plogmaker, J. A. Terschlüsen, N. Krebs, M. Svanqvist, J. Forsberg, U. B. Cappel, J.-E. Rubensson, H. Siegbahn, and J. Söderström, "HELIOS - A laboratory based on high-order harmonic generation of extreme ultraviolet photons for time-resolved spectroscopy," *Rev. Sci. Instrum.*, vol. 86, p. 123107, dec 2015.

[34] R. Stefanuik, R. Knut, S. Jana, J. A. Terschlüsen, A. Sandell, and J. Söderström, "Developments and enhancements to the HELIOS pump probe system," *J. Electron Spectros. Relat. Phenomena*, vol. 224, pp. 33–37, 2018.

[35] R. S. Malik, E. K. Delczeg-Czirjak, R. Knut, D. Thonig, I. Vaskivskyi, D. Phuyal, R. Gupta, S. Jana, R. Stefanuik, Y. O. Kvashnin, S. Husain, A. Kumar, P. Svedlindh, J. Söderström, O. Eriksson, and O. Karis, "Ultrafast magnetization dynamics in the half-metallic Heusler alloy Co2 FeAl," *Phys. Rev. B*, vol. 104, p. L100408, sep 2021.

[36] C. von Korff Schmising, F. Willems, S. Sharma, K. Yao, M. Borchert, M. Hennecke, D. Schick, I. Radu, C. Strüber, D. W. Engel, V. Shokeen, J. Buck, K. Bagschik, J. Viefhaus, G. Hartmann, B. Manschwetus, S. Grunewald, S. Düsterer, E. Jal, B. Vodungbo, J. Lüning, and S. Eisebitt, "Element-Specific Magnetization Dynamics of Complex Magnetic Systems Probed by Ultrafast Magneto-Optical Spectroscopy," *Appl. Sci.*, vol. 10, p. 7580, oct 2020.

[37] I. Vaskivskyi, R. S. Malik, L. Salemi, D. Turenne, R. Knut, J. Brock, R. Stefanuik, J. Söderström, K. Carva, E. E. Fullerton, P. M. Oppeneer, O. Karis, and H. A. Dürr, "Element-Specific Magnetization Dynamics in Co-Pt Alloys Induced by Strong Optical Excitation," *J. Phys. Chem. C*, pp. 125–11714, 2021.

[38] D. Rudolf, C. La-O-Vorakiat, M. Battiato, R. Adam, J. M. Shaw, E. Turgut, P. Maldonado, S. Mathias, P. Grychtol, H. T. Nembach, T. J. Silva, M. Aeschlimann, H. C. Kapteyn, M. M. Murnane, C. M. Schneider, and P. M. Oppeneer, "Ultrafast magnetization enhancement in metallic multilayers driven

by superdiffusive spin current," *Nat. Commun.*, vol. 3, pp. 1–6, sep 2012.

[39] F. Willems, C. von Korff Schmising, C. Strüber, D. Schick, D. W. Engel, J. K. Dewhurst, P. Elliott, S. Sharma, and S. Eisebitt, "Optical inter-site spin transfer probed by energy and spin-resolved transient absorption spectroscopy," *Nat. Commun.*, vol. 11, pp. 1–7, dec 2020.

[40] J. K. Dewhurst, P. Elliott, S. Shallcross, E. K. Gross, and S. Sharma, "Laser-induced intersite spin transfer," *Nano Lett.*, vol. 18, pp. 1842–1848, mar 2018.

[41] M. Hecker, P. M. Oppeneer, S. Valencia, H.-C. Mertins, and C. M. Schneider, "Soft X-ray magnetic reflection spectroscopy at the 3p absorption edges of thin Fe films," *J. Electron Spectros. Relat. Phenomena*, vol. 144-147, pp. 881–884, 2005.

[42] H. C. Kapteyn, M. M. Murnane, and I. P. Christov, "Extreme Nonlinear Optics: Coherent X rays from Lasers," *Phys. Today*, vol. 58, no. 3, pp. 39–46, 2005.

[43] T. Popmintchev, M. C. Chen, A. Paul, M. M. Murnane, and H. C. Kapteyn, "The attosecond nonlinear optics of bright coherent X-ray generation," *Nat. Commun.*, vol. 4, no. 12, pp. 822–832, 2010.

[44] X. He, J. M. Dahlström, R. Rakowski, C. M. Heyl, A. Persson, J. Mauritsson, and A. L'Huillier, "Interference effects in two-color high-order harmonic generation," *Phys. Rev. A*, vol. 82, p. 33410, sep 2010.

[45] S. Jana, J. A. Terschlüsen, R. Stefanuik, S. Plogmaker, S. Troisi, R. S. Malik, M. Svanqvist, R. Knut, J. Söderström, and O. Karis, "A setup for element specific magnetization dynamics using the transverse magneto-optic Kerr effect in the energy range of 30-72 eV," *Rev. Sci. Instrum.*, vol. 88, no. 3, p. 33113, 2017.

[46] A. V. Singh, B. Khodadadi, J. B. Mohammadi, S. Keshavarz, T. Mewes, D. S. Negi, R. Datta, Z. Galazka, R. Uecker, and A. Gupta, "Bulk Single Crystal-Like Structural and Magnetic Characteristics of Epitaxial Spinel Ferrite Thin Films with Elimination of Antiphase Boundaries," *Adv. Mater.*, vol. 29, no. 30, p. 1701222, 2017.

[47] Q.-C. Sun, H. Sims, D. Mazumdar, J. X. Ma, B. S. Holinsworth, K. R. O'Neal, G. Kim, W. H. Butler, A. Gupta, and J. L. Musfeldt, "Optical band gap hierarchy in a magnetic oxide: Electronic structure of NiFe2O4," *Phys. Rev. B*, vol. 86, p. 205106, nov 2012.

[48] H. Perron, T. Mellier, C. Domain, J. Roques, E. Simoni, R. Drot, and H. Catalette, "Structural investigation and electronic properties of the nickel ferrite {NiFe}2O4: a periodic density functional theory approach," *J. Phys. Condens. Matter*, vol. 19, p. 346219, jul 2007.

[49] S. Anjum, G. H. Jaffari, A. K. Rumaiz, M. S. Rafique, and S. I. Shah, "Role of vacancies in transport and magnetic properties of nickel ferrite thin films," *J. Phys. D. Appl. Phys.*, vol. 43, p. 265001, jun 2010.

[50] G. H. Jaffari, A. K. Rumaiz, J. C. Woicik, and S. I. Shah, "Influence of oxygen vacancies on the electronic structure and magnetic properties of NiFe2O4 thin films," *J. Appl. Phys.*, vol. 111, no. 9, p. 93906, 2012.

[51] P. Padmanabhan, F. Sekiguchi, R. B. Versteeg, E. Slivina, V. Tsurkan, S. Bordács, I. Kézsmárki, and

P. H. M. van Loosdrecht, "Optically Driven Collective Spin Excitations and Magnetization Dynamics in the Néel-type Skyrmion Host <math xmlns," *Phys. Rev. Lett.*, vol. 122, p. 107203, mar 2019.

[52] E. Terrier, Y. Liu, B. P. Pichon, S. Bégin-Colin, and V. Halté, "Ultrafast demagnetization in Fe 3 O 4 and gamma-Fe 2 O 3 nanoparticles: the role of enhanced antiferromagnetic exchange interaction," *J. Phys. D. Appl. Phys.*, vol. 49, p. 505001, dec 2016.

[53] T. Kampfrath, A. Sell, G. Klatt, A. Pashkin, S. Mährlein, T. Dekorsy, M. Wolf, M. Fiebig, A. Leitenstorfer, and R. Huber, "Coherent terahertz control of antiferromagnetic spin waves," *Nat. Photonics*, vol. 5, pp. 31–34, jan 2011.

[54] S. Mathias, C. La-O-Vorakiat, P. Grychtol, P. Granitzka, E. Turgut, J. M. Shaw, R. Adam, H. T. Nembach, M. E. Siemens, S. Eich, C. M. Schneider, T. J. Silva, M. Aeschlimann, M. M. Murnane, and H. C. Kapteyn, "Probing the timescale of the exchange interaction in a ferromagnetic alloy.," *Proc. Natl. Acad. Sci. U. S. A.*, vol. 109, pp. 4792–7, mar 2012.

AIP Publishing

Journal of Applied Physics

ACCEPTED MANUSCRIPT

This is the author's peer reviewed, accepted manuscript. However, the online version of record will be different from this version once it has been copyedited and typeset.
PLEASE CITE THIS ARTICLE AS DOI: 10.1063/5.0073606

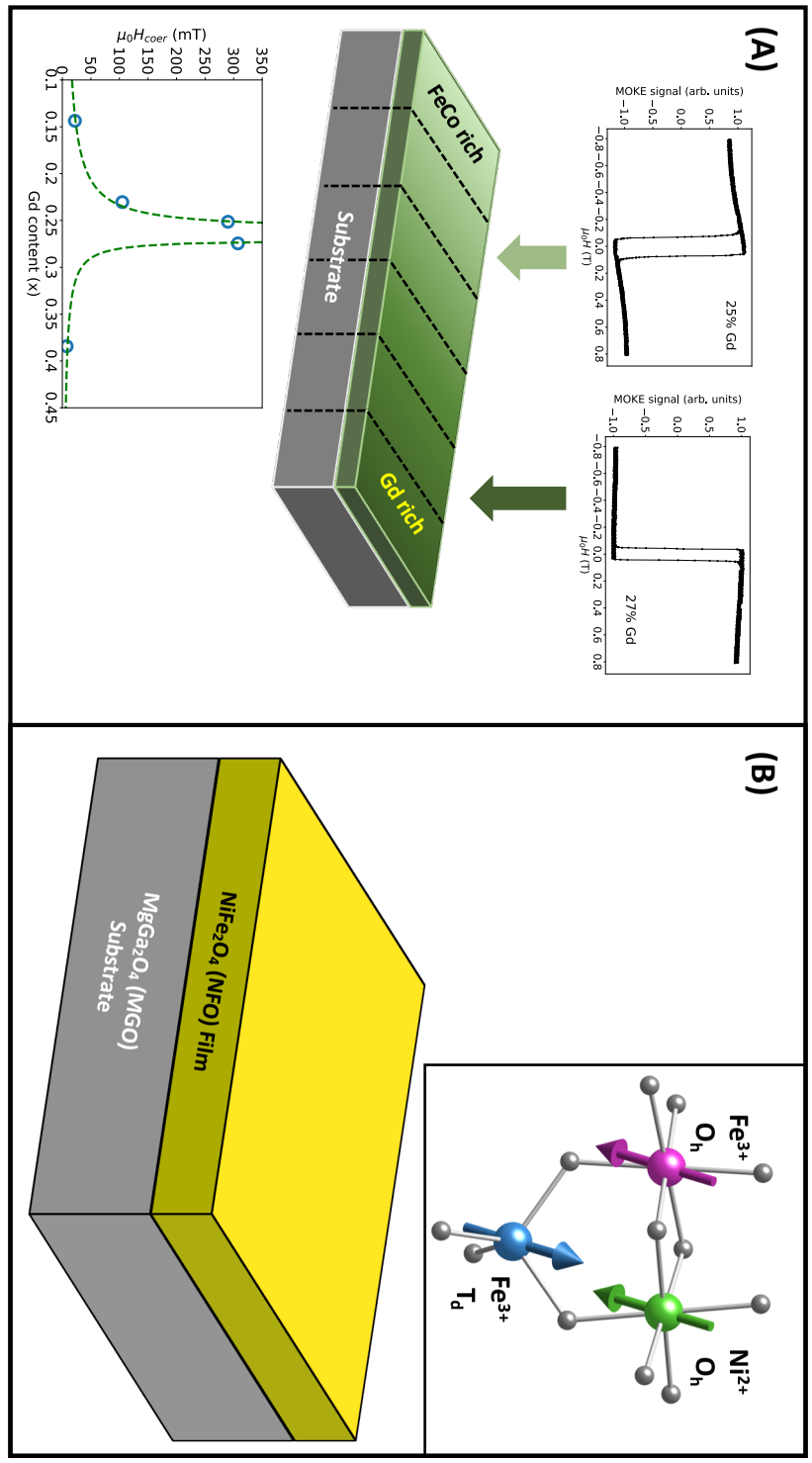

Journal of Applied Physics

PLEASE CITE THIS ARTICLE AS DOI: 10.1063/5.0073606

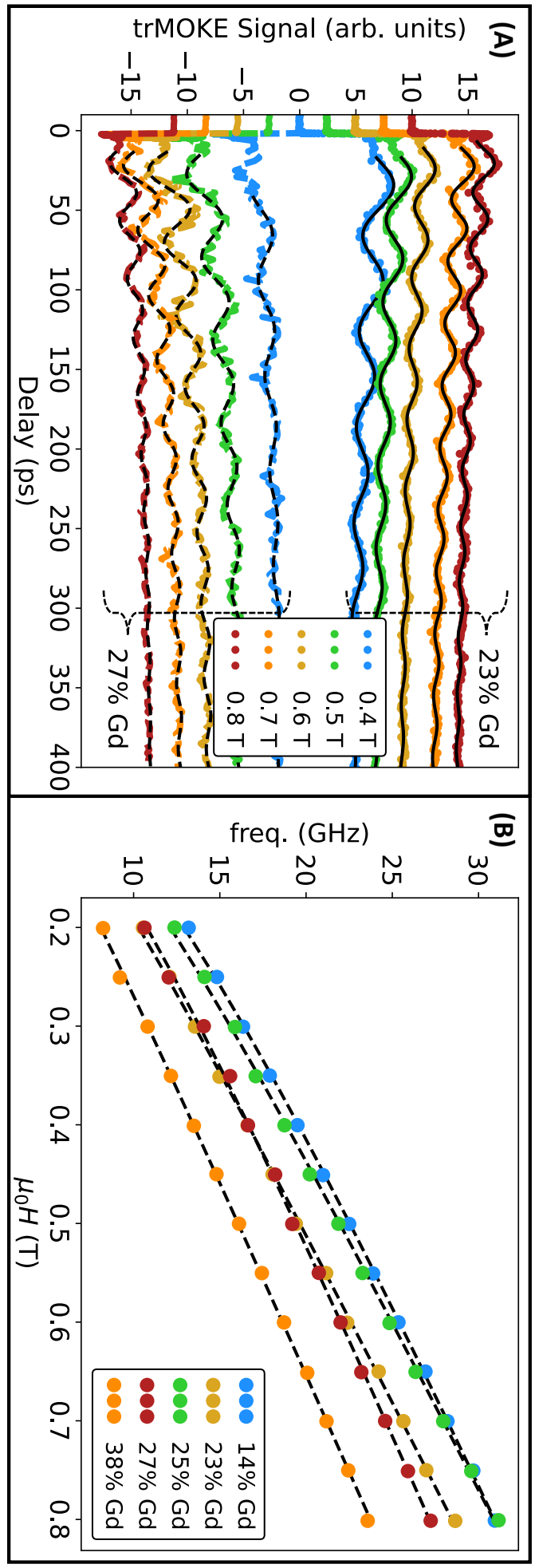

Journal of Applied Physics

PLEASE CITE THIS ARTICLE AS DOI: 10.1063/5.0073606

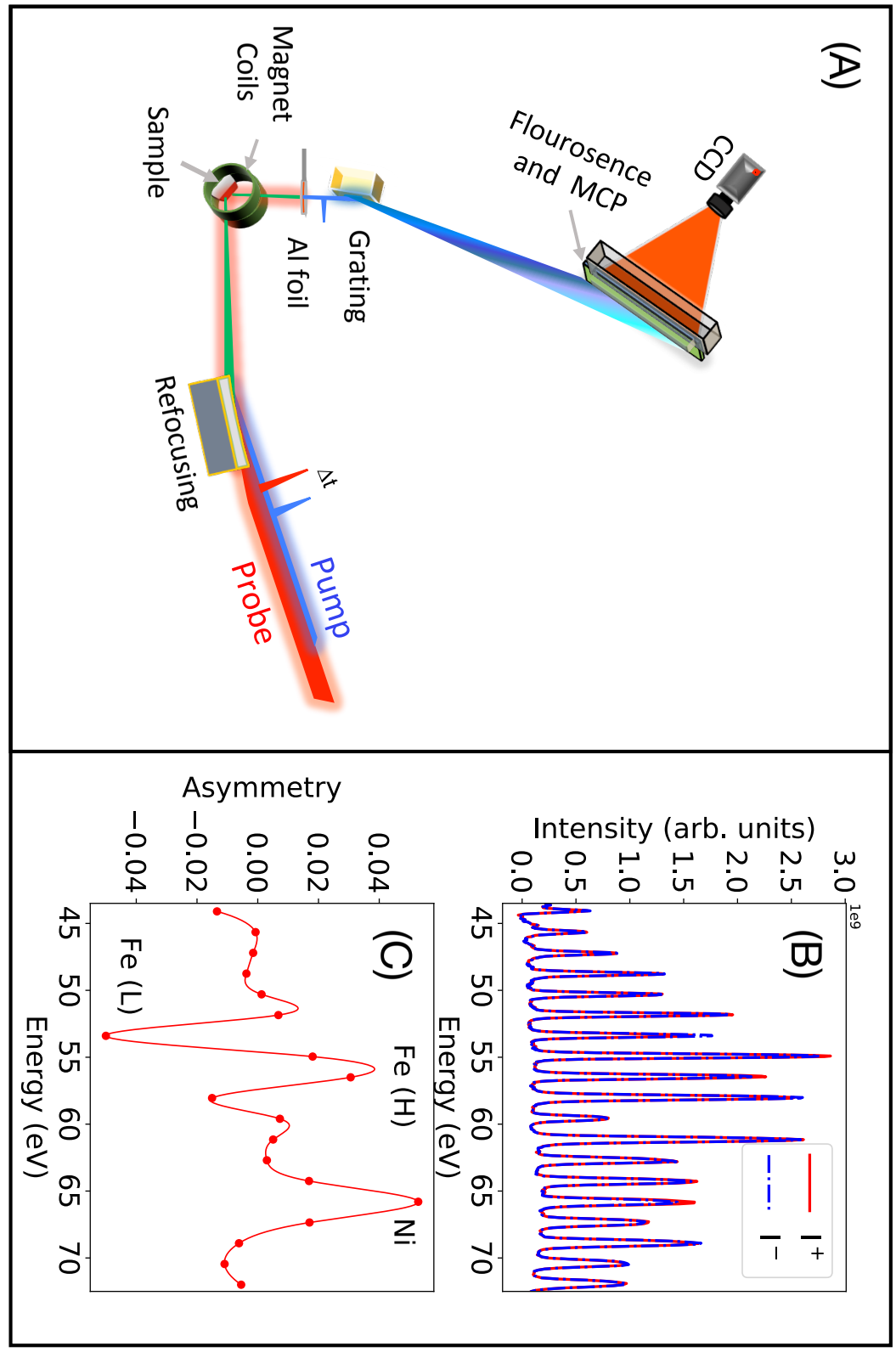

AIP Publishing

Journal of Applied Physics

ACCEPTED MANUSCRIPT

This is the author's peer reviewed, accepted manuscript. However, the online version of record will be different from this version once it has been copyedited and typeset.
PLEASE CITE THIS ARTICLE AS DOI: 10.1063/5.0073606